

PACS numbers: 61.46.Hk, 75.50.Cc, 75.60.Ej, 75.75.-c, 81.20.Fw

## Magnetic Properties of Magnetic Fluids Based on $\text{Ni}_x\text{Co}_{1-x}\text{Fe}_2\text{O}_4$

O. K. Kuvandikov, S. J. Kuvandikov, and K. A. ugli Kayumov

*Samarkand State University,  
15 University Blvd.,  
140104 Samarkand, Uzbekistan*

In this work the magnetic fluids based on  $\text{Ni}_x\text{Co}_{1-x}\text{Fe}_2\text{O}_4$  with  $x = 0, 0.3, 0.5, 0.7, 1$  are obtained by the chemical co-precipitation method. Crystal structure, morphology, elemental composition of the  $\text{Ni}_x\text{Co}_{1-x}\text{Fe}_2\text{O}_4$  nanoparticles and magnetic properties of the magnetic fluids are studied by X-ray diffraction, transmission electron microscope, energy-dispersive X-ray analysis and vibrating sample magnetometer.

**Key words:** magnetic fluid, nanoparticle, magnetometer, energy-dispersive X-ray analysis, ferrite.

У даній роботі магнетні рідини на основі  $\text{Ni}_x\text{Co}_{1-x}\text{Fe}_2\text{O}_4$  з  $x = 0, 0.3, 0.5, 0.7, 1$  було одержано методом хімічного співосадження. Кристалічну структуру, морфологію, елементний склад наночастинок  $\text{Ni}_x\text{Co}_{1-x}\text{Fe}_2\text{O}_4$  і магнетні властивості магнетних рідин вивчали за допомогою рентгенофазового аналізу, просвічувального електронного мікроскопа, енергодисперсійного рентгенівського аналізу і вібраційного магнітометра.

**Ключові слова:** магнетна рідина, наночастинка, магнетометр, енергодисперсійний рентгенівський аналіз, ферит.

*(Received June 18, 2020; in final version, September 24, 2020)*

---

Corresponding author: Oblakul Kuvandikovich Kuvandikov  
E-mail: [quvandikov@rambler.ru](mailto:quvandikov@rambler.ru)

Citation: O. K. Kuvandikov, S. J. Kuvandikov, and K. A. ugli Kayumov,  
Magnetic Properties of Magnetic Fluids Based on  $\text{Ni}_x\text{Co}_{1-x}\text{Fe}_2\text{O}_4$ ,  
*Metallofiz. Noveishie Tekhnol.*, **42**, No. 11: 1499–1507 (2020),  
DOI: [10.15407/mfint.42.11.1499](https://doi.org/10.15407/mfint.42.11.1499).

## 1. INTRODUCTION

Nowadays, the physical properties of the magnetic fluids based on ferrites containing 3d metals nanoparticles are being studied with great interest. Also, due to the breadth of the field of application, methods of obtaining these materials are evolving [1, 2]. Magnetic fluids are a colloidal solution composed of ferro or ferrimagnetic nanoparticles stabilized in a carrier liquid [3]. Due to the unique physical properties of such liquids, they are using in medicine, electronics, industry mining, machinery and other fields [4, 5]. The technological process of the preparation of magnetic fluids consists of two stages [6]. The first is the synthesis of magnetic nanoparticles. The second is the stabilization of the synthesized nanoparticles in a carrier liquid by surfactants or polymers [7]. As of today, there is a variety of methods to synthesize magnetic nanoparticles such as co-precipitation, hydrothermal, sol-gel, thermal decomposition, solvothermal, sonochemical, electrochemical, mechanical milling and other methods [5, 8, 9]. In the synthesis of the  $\text{Ni}_x\text{Co}_{1-x}\text{Fe}_2\text{O}_4$ , the chemical co-precipitation method was acceptable to us because for its simplicity, convenience, low cost, and most importantly, the ability to control the size of the particles. To prevent the formation of aggregates nanomagnetic particles of magnetic fluid the surfactant is used. Generally, surfactant molecules have a polar ‘head’ and a non-polar ‘tail’ (or *vice versa*). One of the ends is adsorbed to the particle, and the other is attached to the molecules of the carrier liquid, forming a normal or reverse micelle around the particle respectively [10]. We used sodium oleate as a surfactant in the preparation of the liquids.

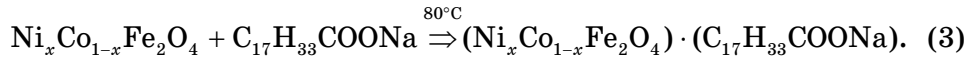
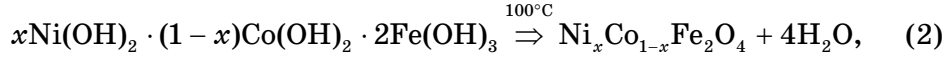
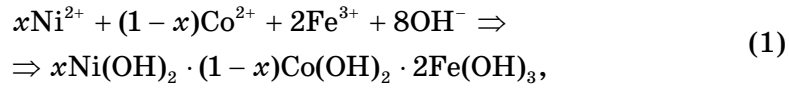
Studies have demonstrated that ferrite particles with the general formula  $\text{Ni}_x\text{Co}_{1-x}\text{Fe}_2\text{O}_4$  have superparamagnetic nature at a size of 15–20 nm [11–13]. The crystal structure of  $\text{Ni}_x\text{Co}_{1-x}\text{Fe}_2\text{O}_4$  is cubic spinel ferrite of the  $Fd3m$  space group [14]. Experiments have shown that an increase in the concentration of Ni ions in  $\text{Ni}_x\text{Co}_{1-x}\text{Fe}_2\text{O}_4$  affecting its physical properties in general [15].

The aim of this research work is to synthesis to the magnetic fluids based on single-phase nickel-doped cobalt ferrite nanoparticles and to studying their crystal structure, morphology, element composition, and magnetization.

## 2. MATERIALS AND METHODS

In the preparation of the magnetic fluids, initially, their ferrophase  $\text{Ni}_x\text{Co}_{1-x}\text{Fe}_2\text{O}_4$  with various concentrations of nickel ions  $x = 0, 0.3, 0.5, 0.7, 1$  have been synthesized by the chemical co-precipitation method. Each of the salts of  $\text{Fe}(\text{NO}_3)_3 \cdot 9\text{H}_2\text{O}$ ,  $\text{Co}(\text{NO}_3)_2 \cdot 6\text{H}_2\text{O}$ ,  $\text{Ni}(\text{NO}_3)_2 \cdot 6\text{H}_2\text{O}$  with the molar ratio of  $\text{Ni}^{2+} : \text{Co}^{2+} : \text{Fe}^{3+} = x : (1 - x) : 2$  were dissolved sepa-

rately in 100 ml of double distilled water. The resulting product (or solutions) together mixed at 60°C using a magnetic stirrer for 30 min. Afterward 1M NaOH as the precipitating agent was slowly added to the resulting salt solution drop by drop until the pH = 10 and stirred at 100°C 1 hours. Thereafter, the metal ions are converted into hydroxides, and then under the influence of temperature, the hydroxides are transformed into ferrites (Eqs. (1), (2)) [16]. Then the precipitated nanoparticles were washed with double-distilled water several times to remove the impurities. The sediment was filtered and dried in the oven at 200°C for 12 h also pulverized and named as P<sub>1</sub>, P<sub>2</sub>, P<sub>3</sub>, P<sub>4</sub>, P<sub>5</sub> according to  $x = 0, 0.3, 0.5, 0.7$ , respectively. For the preparation of magnetic fluids 1 g of sodium oleate dissolved in 50 ml of distilled water was added to the sediment as a surfactant to prevent particle agglomeration, then mixed well at 80°C for 1 h (Eq. (3)). The reaction equation of the experiment is shown below:



The magnetic fluids of concentration 1% vol. based on  $\text{Ni}_x\text{Co}_{1-x}\text{Fe}_2\text{O}_4$  nanoparticles with Ni doping concentration  $x = 0, 0.3, 0.5, 0.7, 1$  are assigned with sample codes MF1, MF2, MF3, MF4 and MF5, respectively.

Structural and phase analysis of the P<sub>1</sub>, P<sub>2</sub>, P<sub>3</sub>, P<sub>4</sub>, P<sub>5</sub> powder samples were studied by the using XRD Empyrean Panalalytical ( $\text{CuK}_\alpha$  radiation  $\lambda = 0.15406$  nm, for  $2\theta$  values ranging from 10° to 80°) diffractometer. Morphological of the nanoparticles of the magnetic fluids and elemental composition of the powders have been examined using a transmission electron microscope (model: TEM LEO 912 AB) and an energy dispersive X-ray spectroscopy (EDX, model: X-ACT Silicon Drift Detector). The magnetizations of the MF1, MF2, MF3, MF4 and MF5 samples were measured with a VSM magnetometer at the room temperature.

### 3. RESULTS AND DISCUSSION

#### 3.1. X-Ray Diffraction Analysis

XRD patterns of the synthesized P<sub>1</sub>, P<sub>2</sub>, P<sub>3</sub>, and P<sub>4</sub> samples are shown in Fig. 1. All the diffraction peaks of the patterns show that the single-

phase cubic spinel crystal structure is formed and is well compatible with the JCPDS cards 742081 for  $\text{NiFe}_2\text{O}_4$  and 791744 for  $\text{CoFe}_2\text{O}_4$ . Also, there are no impurities in the patterns indicating that the successful synthesis of cubic spinel ferrite crystal structural nickel doped cobalt ferrites belongs to the  $Fd\bar{3}m$  space group. Similar findings can be found in the Refs. [17], [18] for the crystal structure of nickel doped cobalt ferrite synthesized by chemical co-precipitation method. The average crystallite size of the samples has been calculated from the strongest (311) peak of the XRD pattern by using the Debay–Sherrer equation [19]:

$$D = \frac{0.9\lambda}{\beta \cos \theta}. \quad (4)$$

Here,  $\lambda$  is the  $\text{CuK}\alpha$  radiation wavelength for the XRD,  $\beta$  is the width of the half maximum intensity of the peak,  $\theta$  is the Bragg angle.

Besides, the lattice parameter values of the samples were determined using the following equation:  $a = d_{h,k,l} \sqrt{h^2 + k^2 + l^2}$  here,  $h, k, l$  are Miller indices. X-ray density for each sample was calculated from the formula:  $\rho = 8M / N_A a^3$ , where  $M$  is the molecular weight of the

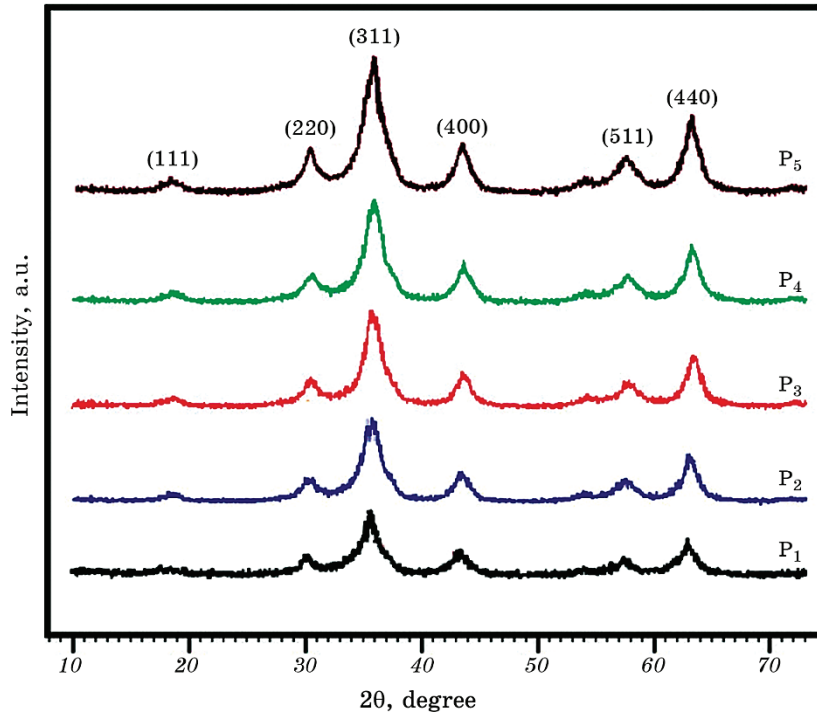


Fig. 1. XRD patterns of the  $P_1$ ,  $P_2$ ,  $P_3$ ,  $P_4$ ,  $P_5$  powders.

**TABLE 1.** Average crystallite size, lattice parameters and X-ray density of the  $\text{P}_1$ ,  $\text{P}_2$ ,  $\text{P}_3$ ,  $\text{P}_4$ ,  $\text{P}_5$  samples.

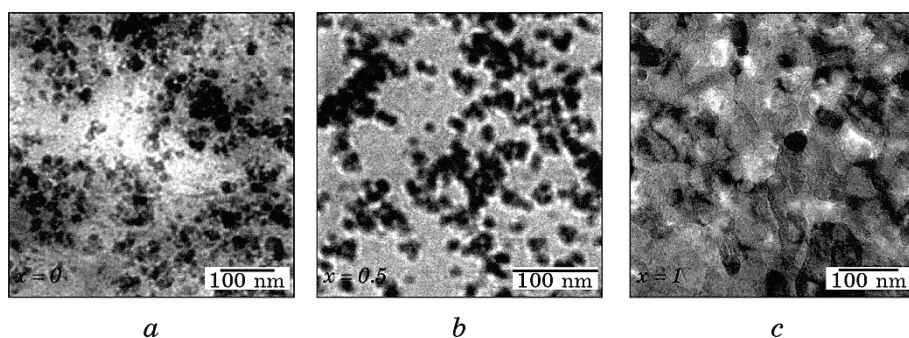
Sample	Average crystallite size (nm)	Lattice parameter (nm)	X-ray density ( $\text{g}/\text{cm}^3$ )
$\text{CoFe}_2\text{O}_4$	21.6	8.365	5.312
$\text{Ni}_{0.3}\text{Co}_{0.7}\text{Fe}_2\text{O}_4$	19.2	8.351	5.324
$\text{Ni}_{0.5}\text{Co}_{0.5}\text{Fe}_2\text{O}_4$	18.9	8.340	5.347
$\text{Ni}_{0.7}\text{Co}_{0.3}\text{Fe}_2\text{O}_4$	15.4	8.335	5.352
$\text{NiFe}_2\text{O}_4$	19.1	8.331	5.381

sample,  $N_A$  is Avogadro constant,  $a$  is the lattice parameter. The obtained results are given in Table 1.

As it can be seen that from Table 1 the average crystallite size varies in the range of 15–22 nm. Lattice parameter of the powdery  $\text{Ni}_x\text{Co}_{1-x}\text{Fe}_2\text{O}_4$  samples decreases with increasing  $\text{Ni}^{2+}$  concentration, but the X-ray density increases. Such changes can be explained by the fact that the  $\text{Ni}^{2+}$  (0.69 Å) ion has a smaller ionic radius than the  $\text{Co}^{2+}$  (0.74 Å) ion [20].

### 3.2. TEM Studies

The shape, size and morphology of the nanoparticles of the M1, M3, M5 samples were investigated using transmission electron microscope (TEM). The obtained results are shown in Fig. 2. From TEM images it can be seen that almost all of the particles of the samples are spherical in shape. Also the average size of the particles are 18, 23, 28 nm with  $x = 0, 0.5, 1$ , respectively.

**Fig. 2.** TEM images of the  $\text{Ni}_x\text{Co}_{1-x}\text{Fe}_2\text{O}_4$  nanoparticles.

### 3.3. Chemical Composition Studies

The elemental compositions of the  $P_1$ ,  $P_2$ ,  $P_3$ ,  $P_4$ ,  $P_5$  were analysed by the energy dispersive X-ray (EDX) measurements. The measurement results are shown in Fig. 3. As can be seen from the Fig. 3 the presence of Fe, Co, Ni and O elements in the all samples and weight percentage values of the Fe and O are higher than Ni and Co.

### 3.4. Magnetic Properties

The dependence of the specific magnetization of the M1, M2, M3, M4 and

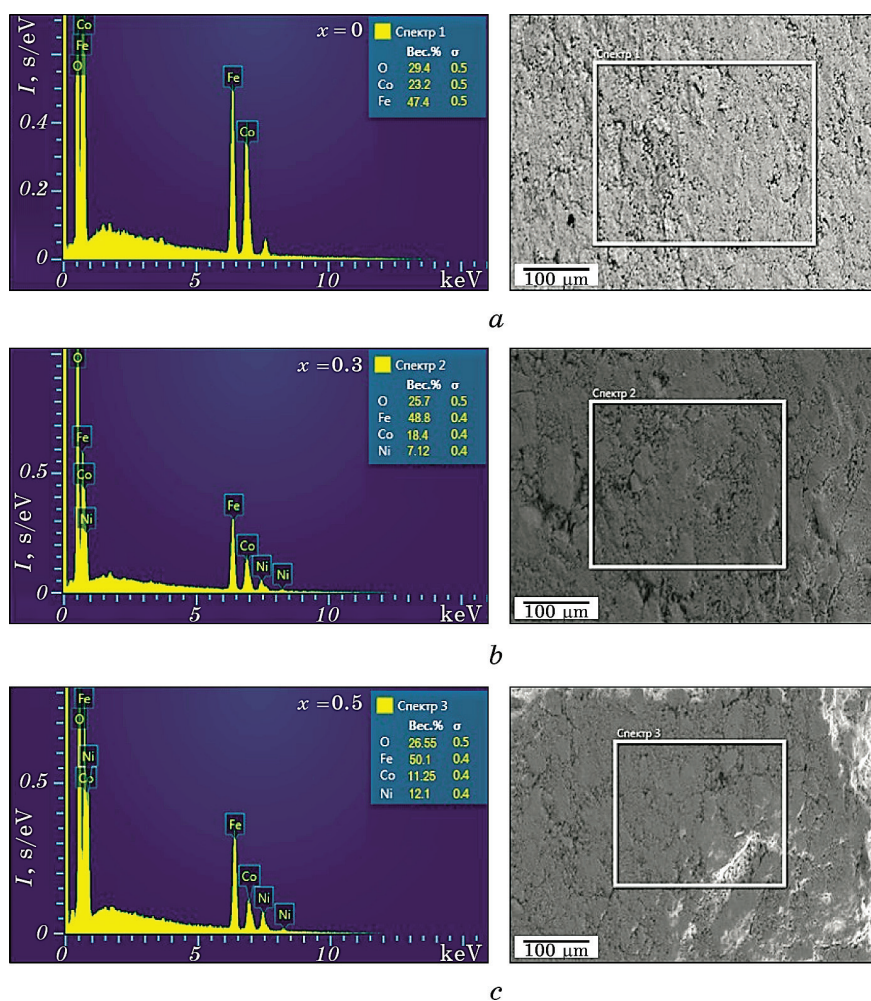
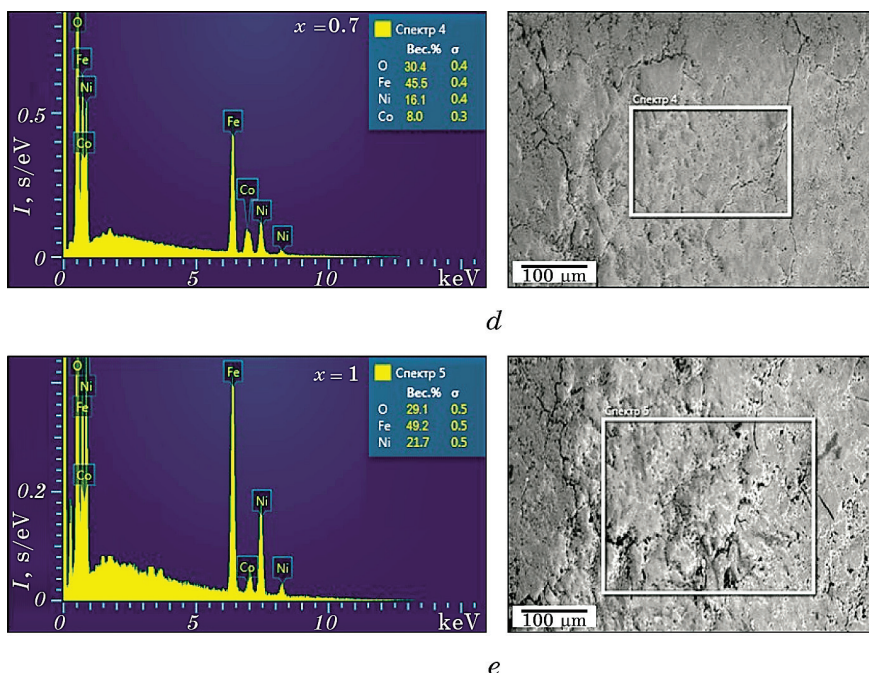


Fig. 3. EDX spectra of all the powders.





Continuation of the Fig. 3.

M5 magnetic fluids of concentration 1% vol. of  $\text{Ni}_x\text{Co}_{1-x}\text{Fe}_2\text{O}_4$  on the magnetic field was measured at the room temperature by VSM. The results of the measurements are shown in Fig. 4. We can see from Fig. 4 the magnetization of the samples increases with increasing magnetic field and attains the saturation. From the magnetization hysteresis loops of the Fig. 4 we can determine the saturation magnetization, remnant magnetization and the coercivity values and these values are shown in Table 2. Based on the results in Table 2. It can be said the saturation magnetization of the all fluids decreases from 2.9 emu/g to 1.5 emu/g with an increase in nickel ion of the hard phase. Such decreasing in the magnetization of the fluids can be explained by the fact that the magnetic moment of  $\text{Ni}^{2+}$  ( $2\mu_B$ ) is smaller than the magnetic moment of  $\text{Co}^{2+}$  ( $3\mu_B$ ).

#### 4. CONCLUSION

Magnetic fluids based on  $\text{Ni}_x\text{Co}_{1-x}\text{Fe}_2\text{O}_4$  synthesized at different concentrations of nickel were obtained by the chemical co-precipitation method. Based on X-ray diffraction and EDX analysis it was confirmed that the synthesized particles were  $\text{Ni}_x\text{Co}_{1-x}\text{Fe}_2\text{O}_4$ . TEM measurements showed that the average particle size decreased as the proportion of nickel in the samples increased. Magnetic studies have revealed that

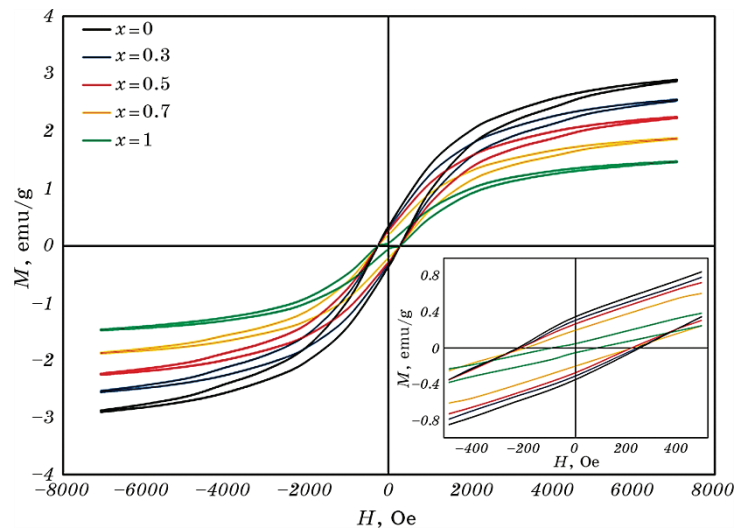


**Fig. 4.** Hysteresis loops of the magnetic fluids based on  $\text{Ni}_x\text{Co}_{1-x}\text{Fe}_2\text{O}_4$ .

**TABLE 2.** Magnetic properties of magnetic fluids: saturation magnetization ( $M_s$ ), remanent magnetization ( $M_r$ ), coercivity ( $H_c$ ).

Samples	$M_s$ (emu/g)	$M_r$ (emu/g)	$H_c$ (Oe)
M1 (magnetic fluid of concentration 1% vol. of the $\text{CoFe}_2\text{O}_4$ )	2.9	0.35	210
M2 (magnetic fluid of concentration 1% vol. of the $\text{Ni}_{0.3}\text{Co}_{0.7}\text{Fe}_2\text{O}_4$ )	2.5	0.31	250
M3 (magnetic fluid of concentration 1% vol. of the $\text{Ni}_{0.5}\text{Co}_{0.5}\text{Fe}_2\text{O}_4$ )	2.26	0.27	220
M4 (magnetic fluid of concentration 1% vol. of the $\text{Ni}_{0.7}\text{Co}_{0.3}\text{Fe}_2\text{O}_4$ )	1.89	0.22	140
M5 (magnetic fluid of concentration 1% vol. of the $\text{NiFe}_2\text{O}_4$ )	1.5	0.05	100

the magnetic fluids of the same concentration show superparamagnetic nature and the saturation magnetization of the fluids decreases with increasing concentration of Ni in  $\text{Ni}_x\text{Co}_{1-x}\text{Fe}_2\text{O}_4$ .

## REFERENCES

1. Vishal K Chakradhary, Azizurrahman Ansari, and M Jaleel Akhtar, *J. Magn. Magn. Mater.*, **469**: 674 (2018).
2. Ya Tang, Xinwei Wang, Qinghong Zhang, Yaogang Li, and Hongzhi Wang,



- Prog. Natural Sci.: Materials International*, **22**, Iss. 1: 53 (2012).
3. S. Taketomi and S. Tikadzumi, *Magnetic Fluids* (Moscow: Mir: 1993), p. 125 (in Russian).
4. Ibrahim Sharifi, H. Shokrollahi, and S. Amiri, *J. Magn. Magn. Mater.*, **324**: 903 (2012).
5. Kebede K. Kefeni, A. M. Titus Msagati, and Bhekie B. Mamba, *Mater. Sci. Eng. B*, **215**: 37 (2017).
6. Ladislau Vekas, Doina Bica, and Mikhail V. Avdeev, *China Particuology*, **5**: 43 (2007).
7. C. Scherer and A. M. Figueiredo Neto, *Braz. J. Phys.*, **35**, No. 3A: 718 (2005).
8. M. Nabeel Rashin and J. Hemalatha, *Ultrasonics*, **54**: 834 (2014).
9. Tetiana Tatarchuk, Mohamed Bououdina, J. Judith Vijaya, and L. John Kennedy, *Spinel Ferrite Nanoparticles: Synthesis, Crystal Structure, Properties, and Perspective Applications* (Springer International Publishing AG: 2017).
10. S. A. Novopashin, M. A. Serebryakova, and S. Ya. Khmel, *Thermophysics and Aeromechanics*, **22**, 397 (2015).
11. Dong-Sik Bae, Sang-Woo Kim, Hae-Weon Lee, and Kyong-Sop Han, *Mater. Lett.*, **57**: 1997 (2003).
12. U. Wongpratrat, S. Maensiri, and E. Swatsitang, *Appl. Surf. Sci.*, **380**: 60 (2016).
13. Bongani Ndlovu, Justice Zakhele Msomi, and Thomas Moyo, *J. Alloys Compd.*, **745**: 187 (2018).
14. Ashwini Kumar, Poorva Sharma, and Dinesh Varshney, *Ceramics International*, **40**: 12855 (2014).
15. Seema Joshi and Manoj Kumar, *Ceramics International*, **42**: 18154 (2016).
16. Ashok Kumar, Nisha Yadav, Dinesh S. Rana, Parmod Kumar, Manju Arora, and R. P. Pant, *J. Magn. Magn. Mater.*, **394**: 379 (2015).
17. K. Maaz, W. Khalid, A. Mumtaz, S. K. Hasanain, J. Liu, and J. L. Duan, *Physica E*, **41**, Iss. 1: 593 (2009).
18. Xuan Zhao, Yue Fu, Jin Yujiao Xu, Jing-Hua Tian, and Ruizhi Yang, *Electrochimica Acta*, **201**: 172 (2016).
19. S. R. Gibin and P. Sivagurunathan, *J. Mater. Sci.: Mater. Electron.*, **28**: 1985 (2017).
20. Ali A. Ati, Zulkafli Othaman, and Alireza Samavati, *J. Molecular Structure*, **1052**: 177 (2013).